Applied Meteorology Unit (AMU)

Quarterly Report

Fourth Quarter FY-02

Contract NAS10-01052

31 October 2002

Distribution

NASA HQ/M/F. Gregory
NASA KSC/AA/R. Bridges
NASA KSC/MK/J. Halsell
NASA KSC/PH/D. King
NASA KSC/PH/E. Mango
NASA KSC/PH/M. Leinbach
NASA KSC/PH/M. Wetmore
NASA KSC/PH-A/J. Guidi
NASA KSC/YA/J. Heald
NASA KSC/YA-C/D. Bartine
NASA KSC/YA-D/H. Delgado
NASA KSC/YA-D/J. Madura
NASA KSC/YA-D/F. Merceret
NASA JSC/MA/R. Dittemore
NASA JSC/MS2/C. Boykin
NASA JSC/ZS8/F. Brody
NASA JSC/ZS8/R. Lafosse
NASA MSFC/ED03/S. Pearson
NASA MSFC/ED41/W. Vaughan
NASA MSFC/ED44/D. Johnson
NASA MSFC/ED44/B. Roberts
NASA MSFC/ED44/S. Deaton
NASA MSFC/MP01/A. McCool
NASA MSFC/MP71/S. Glover
45 WS/CC/N. Wyse
45 WS/DO/P. Broll
45 WS/DOR/S. Cabosky
45 WS/DOR/J. Moffitt
45 WS/DOR/J. Sardonia
45 WS/DOR/J. Tumbiolo
45 WS/DOR/ K. Winters
45 WS/DOR/J. Weems
45 WS/SY/D. Harms
45 WS/SYR/W. Roeder
45 WS/SYA/B. Boyd
45 OG/CC/C. Bowser
45 LG/CC/B. Presley

45 LG/LGP/R. Fore
45 SW/SESL/D. Berlinrut
CSR 4140/H. Herring
CSR 7000/M. Maier
SMC/CWP/G. Deibner
SMC/CWP/T. Knox
SMC/CWP/R. Bailey
SMC/CWP (PRC)/P. Conant
Hq AFSPC/DORW/R. Thomas
Hq AFWA/CC/C. French
Hq AFWA/DNX/E. Bensman
Hq AFWA/DN/N. Feldman
Hq USAF/XOW/H. Tileston
NOAA "W/NP"/L. Uccellini
NOAA/OAR/SSMC-I/J. Golden
NOAA/NWS/OST12/SSMC2/J. McQueen
NOAA Office of Military Affairs/M. Weadon
NWS Melbourne/B. Hagemeyer
NWS Southern Region HQ/"W/SRH"/X. W. Proenza
NWS Southern Region HQ/"W/SR3"/D. Smith
NWS/"W/OSD5"/B. Saffle
NSSL/D. Forsyth
FSU Department of Meteorology/P. Ray
NCAR/J. Wilson
NCAR/Y. H. Kuo
30 WS/SY/C. Crosiar
30 WS/CC/P. Boerlage
30 SW/XP/J. Hetrick
NOAA/ERL/FSL/J. McGinley
Office of the Federal Coordinator for Meteorological
    Services and Supporting Research
Boeing Houston/S. Gonzalez
Aerospace Corp/T. Adang
Yankee Environmental Systems, Inc./B. Bauman
Lockheed Martin Mission Systems/T. Wilfong
ACTA, Inc./B. Parks
ENSCO, Inc./E. Lambert

EXECUTIVE SUMMARY

This report summarizes the Applied Meteorology Unit (AMU) activities for the fourth quarter of Fiscal Year 2002 (July – September 2002). A detailed project schedule is included in the Appendix.

All AMU personnel attended the AMU Tasking and Prioritization Meeting on 2 July at the ENSCO, Inc. office in Melbourne, FL. Participating agencies included SMG, 45 WS, NWS MLB, and the KSC Weather Office. Of the 11 proposed tasks, the Tasking Group unanimously accepted 9 as the consensus tasking for the next 4 quarters. A summary of the new tasks to be executed by the AMU is given in the table below. Significant progress on the current AMU tasks is given after the table.

Task Name	Product Sought	Operational Benefit	Target Begin Date	Target End Date
Mini-SODAR Evaluation	– Evaluation of SLC-37 Mini-SODAR performance based on data from nearest tall wind tower	– Improved understanding of Mini-SODAR capabilities and limitations for evaluation of Launch Commit Criteria	Aug 02	Sep 03
Improve Anvil Forecasting Phase III	– An operational tool to depict anvil threat sectors based on forecast upper-level winds	– Improved capability for forecasters to anticipate the sector from which anvil clouds may threaten launch, landing, and ground operations	Aug 02	Dec 02
Extend AMPS Moisture Analysis	– Quantitative comparison of AMPS/MSS differences in RH and impact on atmospheric stability indices	– Understanding the impact of the transition to AMPS on operational thunderstorm forecasting indices	Aug 02	Apr 03
Objective Lightning Probability	– A PC-based tool that will provide lightning occurrence probability for the day during the warm season	– This tool will add objectivity to the daily forecast thunderstorm probability value	Jan 03	Mar 04
Extend Statistical Forecast Guidance to the SLF Towers	– Climatologies and distributions of 10-minute peak winds at the SLF wind towers – PC-based GUI tool to retrieve probabilities of exceeding peak speeds of operational interest	– Knowledge of 10-minute peak wind behavior that will assist in making peak wind forecasts for landing operations – Quick access to the climatologies and probability distributions	Jul 02	Jun 03
Real-Time Model Verification	– GUI for AWIPS that will plot time series of point forecasts from available operational models, along with observations	– Shows forecasters which model is performing best – Easy-to-use GUI that can be implemented into existing operational systems	Oct 02	Oct 03
LDIS Optimization and Training Extension	– Expanded analysis domain and improved first-guess fields – Additional data ingestion into the real-time LDIS at NWS MLB – Training on system maintenance	– Increased robustness of the real-time grid analyses – Data-sharing capability with nearby NWS offices – Preparation of analyses for initializing local, high-resolution numerical forecasts	Sep 02	Dec 02
Near Storms Environment	– Assistance in moving graphics generation to separate workstation at NWS MLB – Enhanced / additional severe-weather products	– Reduced workload of current LDIS workstation – Improved analysis products for assessing severe-weather threats	Sep 02	Dec 02

Task	Statistical Short-Range Forecast Tools

Goal Develop a short-range peak winds forecast tool to use in launch/landing support operations.

Milestones Conducted tests to determine the validity of the modeled peak wind speed distributions. Completed a first draft of the Phase I final report. Began work on Phase II by calculating climatologies and distributions of 10-minute peak winds at the SLF towers.

Discussion The results from the tests of the validity of modeled peak wind distributions were inconclusive. Therefore, only the distributions for average speeds with > 600 observations are recommended for operations. The climatologies and distributions of the 10-minute peaks were similar to the 5-minute peaks with one exception: the 10-minute peaks are gamma distributed.

Task	Land Breeze Forecasting

Goal Develop rules of thumb that will improve the reliability of the land-breeze occurrence forecasts and help determine land-breeze timing, and direction.

Milestones Developed forecast guidance for land-breeze occurrence, onset time, and movement. Completed a draft of the final report.

Discussion Mr. Case developed a flowchart to assist forecasters in determining the likelihood of land breeze occurrence in all months, a set of tables that summarizes the statistical properties of land-breeze timing based on surface weather features, and a set of diagrams that provide information about the most likely land-breeze direction in a variety of weather scenarios.

Task	Improve Anvil Forecasting Phase III

Goal Develop a utility that will create and display an Anvil Threat Sector using upper-level wind data from either the ETA or MRF forecast model point data.

Milestones Completed development of the utility, which uses the most current data from either forecast model and displays the forecast Anvil Threat sector valid from 1 - 72 hours.

Discussion The model-based Anvil Threat Sector utility was sent to SMG for their review and was also shown it to several 45 WS LWOs.

Task	Extend AMPS Moisture Profiles

Goal Evaluate differences in moisture profiles between the Automated Meteorological Profiling System (AMPS) and the Meteorological Sounding System (MSS), and determine the impact of those differences on thunderstorm forecasting indices.

Milestones Began analysis of an additional 20 dual-sensor AMPS/MSS profiles taken during the warm season in July and August 2002.

Discussion The comparison of the warm-season AMPS and MSS RH profiles confirms the bias pattern found in the cool season data. The bias pattern makes the atmosphere appear less stable when using thunderstorm forecasting indices created with the AMPS data.

Task	MiniSODAR Evaluation

Goal Compare wind data from the Doppler miniSODAR™ System (DmSS) near SLC-37 to wind data from the nearest tall tower, and determine the reliability and quality of the DmSS data.

Milestones Began acquisition of data from the DmSS and Towers 0006 and 0108 in August, and began comparative analysis in September.

Discussion A preliminary analysis shows the ability of the DmSS data to detect sea breeze passages. However, high wind speed outliers were found in the data after the instrument had operated for several months without maintenance.

Table of Contents

SPECIAL NOTICE TO READERS

Applied Meteorology Unit (AMU) Quarterly Reports are now available on the Wide World Web (WWW) at http://science.ksc.nasa.gov/amu/home.html.

The AMU Quarterly Reports are also available in electronic format via email. If you would like to be added to the email distribution list, please contact Ms. Winifred Lambert (321-853-8130, lambert.winifred@ensco.com). If your mailing information changes or if you would like to be removed from the distribution list, please notify Ms. Lambert or Dr. Francis Merceret (321-867-0818, francis.merceret-1@ksc.nasa.gov).

BACKGROUND

The AMU has been in operation since September 1991. Tasking is determined annually with reviews at least semi-annually. The progress being made in each task is discussed in this report with the primary AMU point of contact reflected on each task and/or subtask.

AMU ACCOMPLISHMENTS DURING THE PAST QUARTER

SHORT-TERM FORECAST IMPROVEMENT

STATISTICAL SHORT-RANGE FORECAST TOOLS (MS. LAMBERT)

The peak winds near the surface are an important forecast element for both the Space Shuttle and Expendable Launch Vehicle (ELV) programs. As defined in the Shuttle Flight Rules (FR) and the Launch Commit Criteria (LCC), each vehicle has certain peak wind thresholds that cannot be exceeded in order to ensure the safety of that vehicle during launch and landing operations. The 45th Weather Squadron (45 WS) and the Spaceflight Meteorology Group (SMG) indicate that peak winds are a challenging parameter to forecast. The goal of this task is to develop short-range peak-wind forecast tools to be used in support of ELV/Shuttle launches and Shuttle landings. Ms. Lambert is using seven years (January 1995 – December 2001) of 5-minute data from the Kennedy Space Center/Cape Canaveral Air Force Station (KSC/CCAFS) wind tower network and any other appropriate data sets to develop a statistical short-term forecast method for peak winds at the specific tower sites shown in Table 1.

Table 1.   The towers and heights at which peak winds forecasts will be made, and their associated launch or landing operation.

Launch Operation	Tower(s)	Primary Height (ft)	Backup Height (ft)
Shuttle	0393/94, 0397/98	60	N/A
Shuttle (*landing*)	511 / 512 / 513	30	N/A
	313	492	N/A
Atlas	36	90	N/A
Delta	20 / 21	90	54
Titan	1101 / 1102	162	54

Modeled Peak Wind Distributions

In the previous AMU Quarterly Reports (First through Third Quarter FY-02), Ms. Lambert described tests in which she found that the peak speed probability density functions (PDFs) were Weibull distributed. The mu, shape, and scale parameters define a Weibull distribution. The mu parameter is analogous to the mean of the distribution. The shape parameter determines the location of the maximum in the distribution, which shifts to the right as the shape value increases. The effect of the scale parameter is to stretch/compress the distribution horizontally, thereby also compressing/stretching it vertically. She also described the development and showed the results of polynomial regression equations that estimated the Weibull parameters of peak speed distributions for average speeds with less than 600 observations. It was the higher average speeds whose number of observations fell below this threshold value, and the speed at which this first occurred varied with tower and height but ranged between 15 – 20 kts. The Weibull parameters for the speeds with more than 600 observations showed a trend that appeared to be modeled easily by the polynomial equations. The equations were, therefore, subsequently used to estimate the parameters for the higher average speeds with too few observations.

The underlying assumption was that the modeled trend represented what the true trend would be if there were enough observations to define the peak speed distributions. To validate this assumption, modeled parameters were compared against the empirical parameters using two methods: a standard error test and a gust factor test.

Standard Error Test

This test determined if the modeled parameter values were within 2 standard errors (SEs) of the empirical parameter values. When the empirical parameters were calculated, the S-PLUS® software (Insightful Corporation 2000) also output the SEs. The actual equation for the Weibull SE in S-PLUS is very complex, but can still be described generally by the equation

$$\mathrm{SE} = \left(s^2 / n\right)^{1/2},$$

where s is the standard deviation and n is the number of observations. The SE values for the parameters of Tower 0397 in January are shown in Figure 1. The errors are very small where there are a large number of observations, but increase significantly when the number of observations decreases for average speeds above 18 kts where the number of observations begins to fall below 600. The SE values for the Weibull mu and shape parameters are almost identical and much smaller than the Weibull scale SE values. For all towers, SE values for the three parameters were very small for lower average wind speeds where the sample sizes were very large, and larger for the higher average wind speeds where the sample size was very small. This result indicates that sample size had a strong effect on the SE value, as seen in the equation above.
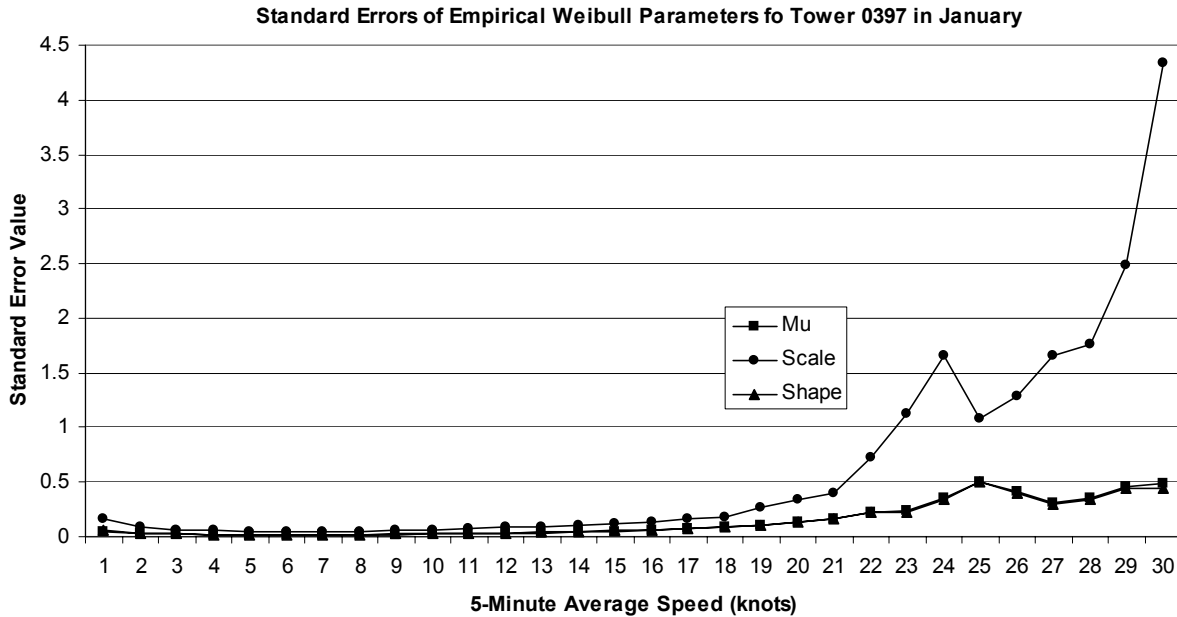
Figure 1.   The standard errors of the empirical Weibull mu, scale and shape parameter values for Tower 397 at 60 ft in January.

Once all modeled parameters, empirical parameters, and SEs were calculated, they were used to check whether the modeled parameters were within 2 SEs of the empirical values. First, the absolute value of the difference between each empirical and modeled parameter value at each average speed was calculated:

$$\text{MuAbsDif} = |\, Mu_E - Mu_M \,|,$$

$$\text{SclAbsDif} = |\, Scl_E - Scl_M \,|, \text{ and}$$

$$\text{ShpAbsDif} = |\, Shp_E - Shp_M \,|,$$

where the subscript E is represents the empirical parameters and the subscript M represents the modeled parameters.

These difference values were then subtracted from a value that was twice the SE of each parameter:

$$\text{MuDif} = 2 * SE_{MU} - \text{MuAbsDif},$$

$$\text{SclDif} = 2 * SE_{SCL} - \text{SclAbsDif, and}$$

$$\text{ShpDif} = 2 * SE_{SHP} - \text{ShpAbsDif.}$$

If the values on the left-hand side of the last three equations were 0 or positive then the modeled parameter values were at or within two SEs of the empirical values. The magnitude showed the extent to which the modeled value was within or outside two SEs of the empirical value.

The values from the last 3 equations are plotted in Figure 2 for each wind speed at Tower 0397 in January. For the average speeds up to 21 kts, the values are small and switch between positive and negative. The SE values for these speeds were all < 0.5 (Figure 1), making it difficult for the modeled values to be within two SEs of the empirical values. Given that the magnitudes of the differences are so small for average speeds less than and including 21 kts in this example, it was assumed that the modeled values were a good approximation for the distributions. Above 21 kts, the magnitudes are larger and most are negative, indicating that the modeled parameter values were outside two SEs. Charts similar to Figure 2 were created for every tower/height/month combination, and showed similar results. This outcome was an indication that the modeled values at the higher speeds were likely incorrect and should not be used for the development of an operational product.
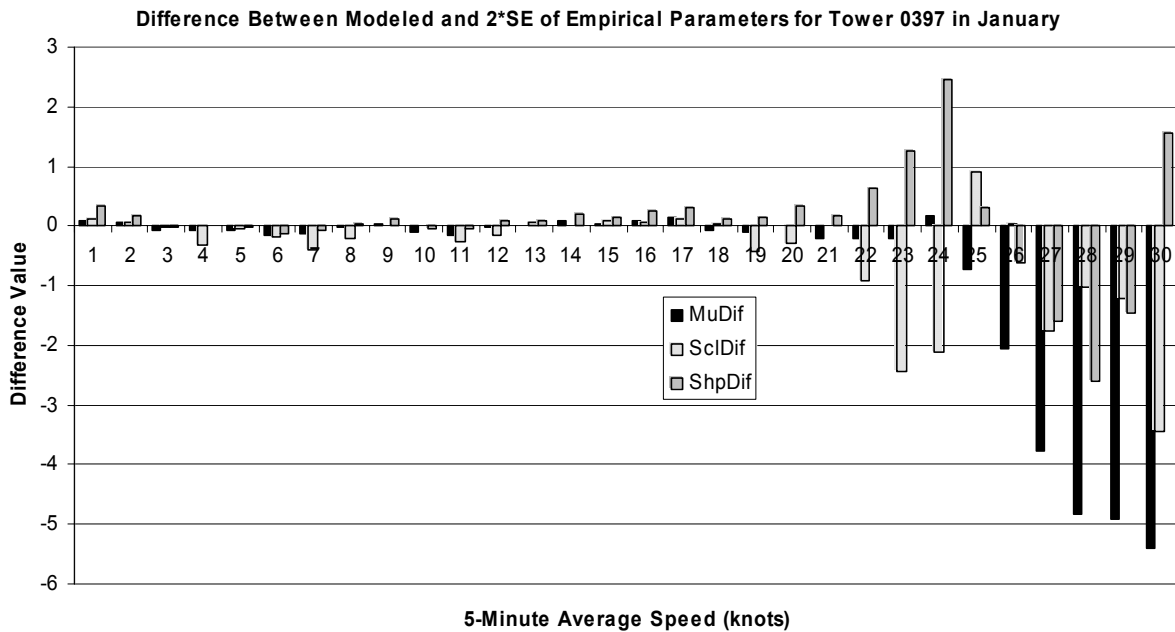
Difference Between Modeled and 2*SE of Empirical Parameters for Tower 0397 in January

Figure 2.   Chart of the differences between 2*SE of the empirical Weibull parameters and the value of the difference between the empirical and modeled parameter values. The differences of each parameter are shown for every 5-minute average speed from Tower 0397 at 60 ft in January.

Gust Factor Test

The gust factor test was done to determine if the modeled parameters produced gust factors (GFs) consistent with known and accepted empirical values (McVehil and Camnitz 1969, NASA 2000, Hsu 2001). Several formulations exist that estimate the gust factor based on average speed, height above ground, and stability. The values in the literature range from 1.2 to 1.6. SMG uses a modified gust factor based on the formulations in McVehil and Camnitz (1969) and NASA (2000). These formulas produce gust factors from 2.5 – 4 at low wind speeds to 1.4 at higher wind speeds. McVehil and Camnitz (1969) showed that the gust factor decreases with increasing average wind speed. In this test, the modeled and empirical mu parameters were used as the peak speed in the gust factor calculation, given that they were considered the mean peak value in the distribution. Gust factors were calculated using the equation

$$GF = Mu / Average\ Speed.$$

The results from the GF calculations for Tower 0397 in January are displayed in Figure 3. All values in the graphs are consistent with those found in the literature. The modeled and empirical GFs are in close agreement from 1 kt up through 20 kts, but begin to diverge at 21 kts. The trends for both GFs decrease to a low point for the lower wind speeds, then increase through 24 kts. The empirical trend tends to 'flatten out' between 10 and 24 kts and then decreases rapidly to 30 kts. The modeled trend continues a smooth increase for all average speeds above 4 kts. The trends for the other tower/month combinations were similar. The modeled GF usually increased with average speed, and the empirical GF tended to be flat and then decrease for the higher average winds.

4

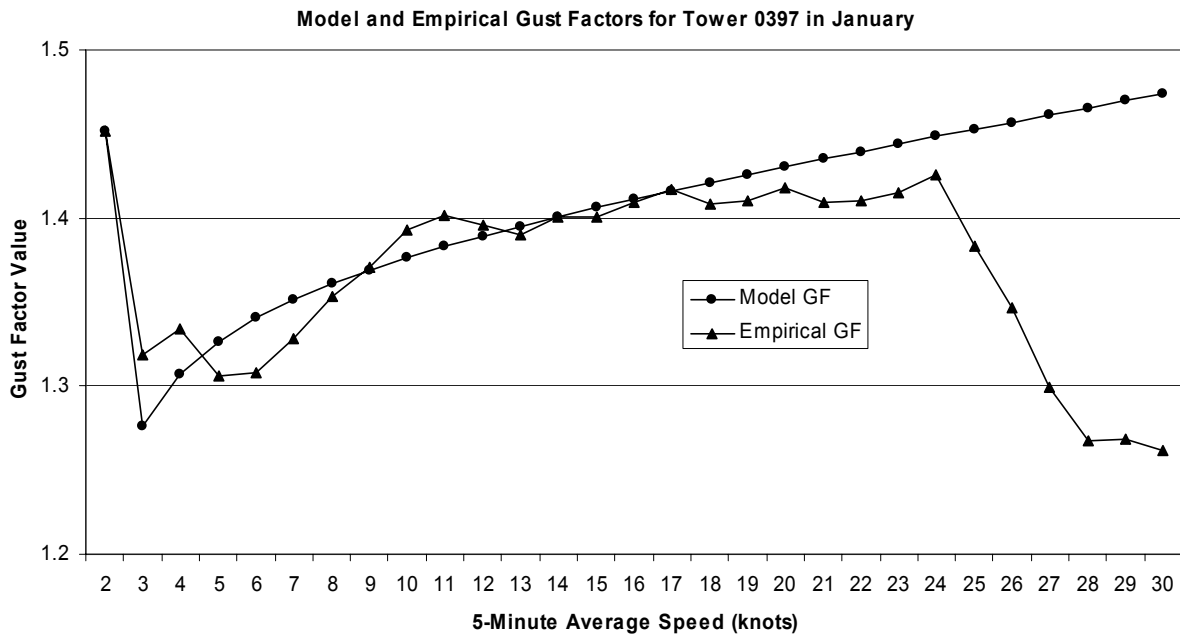**Model and Empirical Gust Factors for Tower 0397 in January**

Figure 3.   The modeled and empirical gust factors for Tower 0397 at 60 ft in January. The modeled and empirical values for the 1-kt average speed are both 2. It is not shown so that the values for the other average speeds could be discerned more easily.

The modeled GF values for the higher wind speeds were most often inconsistent with observed and calculated GF values and trends in the literature. The conclusion from both the SE and GF tests is that the modeled PDFs at higher speeds are likely incorrect and should not be used for the development of an operational product.

Interpretation of Results

Because of the scarcity of observations above ~20 kts average speed for most towers, the validity of modeling the peak speed distributions for these speeds was in question. The standard error and gust factor tests were conducted not as absolute tests, but to produce indications of the soundness of the assumptions that all peak speed distributions were Weibull and that their parameters followed a polynomial trend with average speed. The results from neither test supported the assumptions. It is possible that the Weibull parameters for the peak wind distributions of the higher average speeds do not follow the trend of those for the lower average speeds. It is also possible that the phenomena that create higher average and peak wind speeds produce different theoretical peak wind distributions than Weibull. Regardless of the reason, the distributions for these particular speeds should not be used in operations due to the uncertainty in their accuracy.

Final Report

The final report was in the external review process at the end of the Quarter. The report will be finalized and distributed in October 2002.

For more information on this work, contact Ms. Lambert at 321-853-8130 or lambert.winifred@ensco.com.

LAND BREEZE FORECASTING (MR. CASE AND MR. WHEELER)

The onset of a nocturnal land breeze at KSC, CCAFS, and Patrick Air Force Base is an operationally significant event. The occurrence and timing of the land breeze at night affects low-temperature and fog forecasts, and is critical for toxic material dispersion forecasts during hazardous operations. With current tools, 45 WS forecasters are able to predict the occurrence of a land breeze for a particular night reasonably well, but find it challenging to forecast the timing and direction. As a result, the 45 WS has tasked the AMU to develop forecast rules that will improve the reliability of the occurrence forecasts, and help determine the timing and direction of land-breezes.

In the last AMU Quarterly Report (Third Quarter FY-02), scatter diagrams were shown that demonstrated the relationship between land-breeze onset times and the prevailing surface synoptic flow during October through May in the years 1995 - 2001. Mr. Case expanded the analysis to include the months June through September for both the climatology and the forecast rules. In addition, forecast tools were developed to assist forecasters in predicting the occurrence, timing, and movement of land breezes across east-central Florida.

This section describes the meteorological conditions favorable for a land-breeze occurrence and provides a set of forecast rules that can be applied by forecasters on any given day. The forecast rules were developed from the results of a 7-year climatology (February 1995 to January 2002), and include an analysis of the 300 most distinct land breezes (180 October - May events and 120 June - September events). For each of the events, the Mr. Case examined the mean sea-level pressure field at 0000 UTC on the day of land-breeze occurrence to determine the prevailing low-level synoptic flow across Florida. These large-scale flow characteristics, along with the sea-breeze occurrence/absence during the preceding afternoon, were used to categorize events under various regimes in order to obtain a reliable set of forecast rules. The following sections describe the forecast guidance developed for the land-breeze occurrence, onset time, and direction.

Guidance for Predicting Land-Breeze Occurrence

Figure 4 shows a flowchart that can help determine the likelihood of a land-breeze occurrence during the minimal convective months of October – May (non-convective season). A similar diagram was developed for the peak convective months of June – September (convective season). The logic in the flowchart provides information about the synoptic and mesoscale conditions favorable for the development of a land-breeze front, as well as qualitative and quantitative information on the likelihood of a land breeze occurrence, given existing and forecast meteorological conditions.

The land breeze is a relatively weak mesoscale phenomenon that requires certain meteorological conditions to exist in order for it to develop. These conditions are given at the beginning of the flow chart. For land breeze occurrence, there should be no precipitation across central Florida, mainly clear skies with a general absence of low cloud ceilings for most of the night, average wind speeds at the 54-ft level of the wind towers of less than 7 kts, and the absence of any significant large-scale pressure changes or troughs. A favorable synoptic condition is to have a ridge of high pressure in the vicinity of the Florida peninsula, or a high pressure center overhead. A favorable mesoscale criterion for land-breeze occurrence is to have a sea-breeze circulation during the preceding afternoon. The majority of land breezes during the seven-year data period (57%) occurred after a sea-breeze circulation on the preceding afternoon.

If all initial meteorological criteria are met, the most favorable scenarios for land-breeze occurrence during the non-convective season are found by following the logic in Figure 4. They are:

- Current month from March to May,

- Land breeze during the previous night for November, and March through May (e.g. persistence),

- Sea-breeze occurrence on the previous afternoon in conjunction with offshore synoptic flow,

- Onshore synoptic flow without a sea-breeze during the previous afternoon.

6

Conversely, the least likely scenarios for a land breeze occurrence are:

- Offshore synoptic flow without a sea breeze during the previous afternoon (i.e. synoptic flow is already offshore precluding the development of a land-breeze wind shift),

- Light and variable synoptic flow without a sea breeze during the previous afternoon, or

- Current month is October, December, or January.
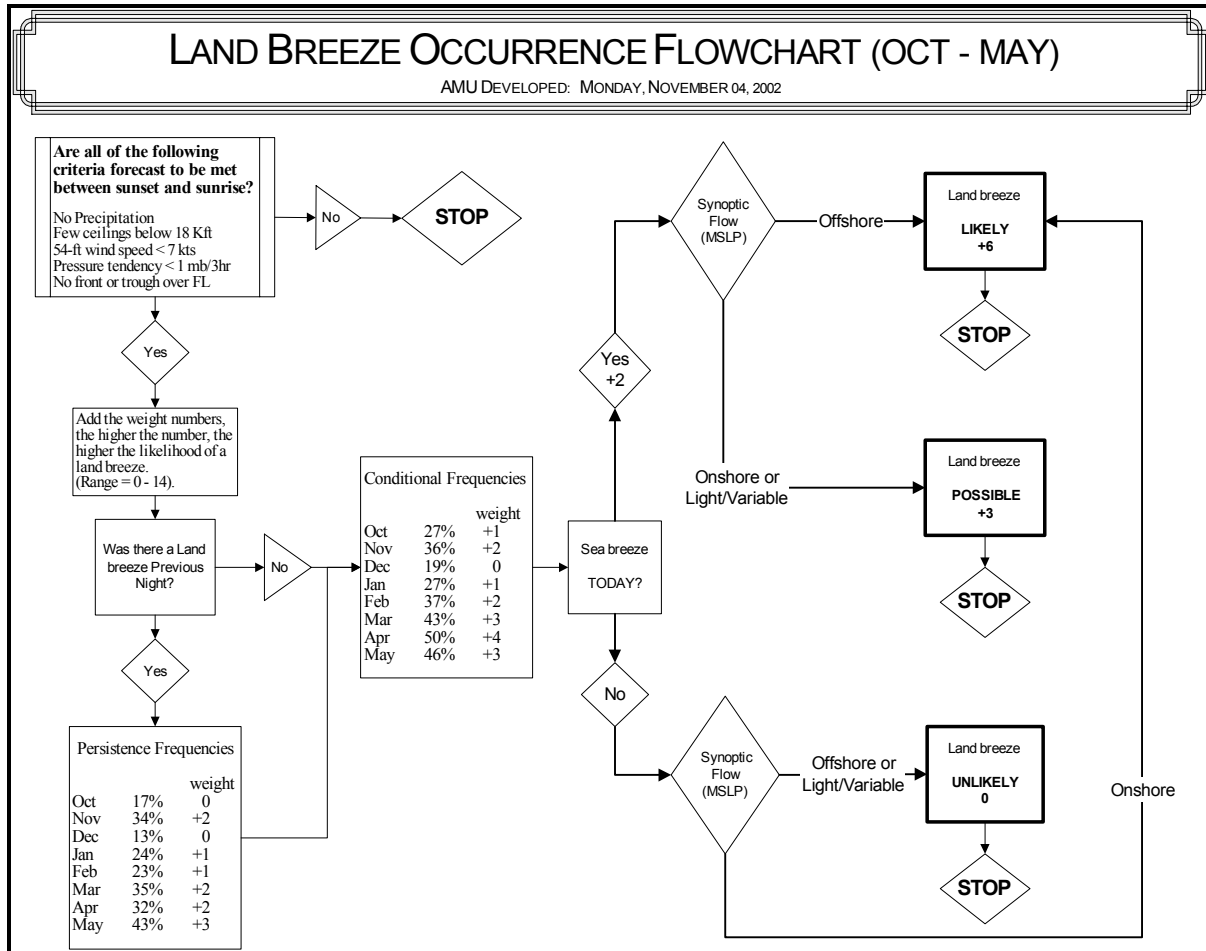
Figure 4. The flowchart for determining the potential of a land-breeze occurrence on any night during the non-convective season. If all of the initial meteorological conditions are met, the forecaster follows the logic of the chart and adds all the weights together. The final number is a qualitative measure of the likelihood of a land breeze occurrence, ranging from 0 (land breeze least likely) to 14 (land breeze most likely). The flowchart also provides the climatological persistence and conditional frequencies for general land-breeze occurrence during each month, provided that all initial meteorological criteria are met.

Guidance for Predicting Land-Breeze Onset Time

Table 2 provides a summary of the statistical distributions of land-breeze onset times based on a clustering of the surface flow regimes and sea-breeze occurrences for the non-convective season. A similar table was developed for the convective season. These tables are designed to provide forecasters with a range of likely onset times based on the time of year, flow regime, and sea-breeze occurrence. The categories with very small sample sizes should be used with caution when determining onset times. In addition, the time ranges should be tuned to the meteorological situation at hand. For example, if the offshore (onshore) surface flow is relatively strong, the forecaster should anticipate an earlier (later) than average onset time of the land breeze. Forecasters should also refer to the mean onset times for each month (not shown) to adjust the predicted times based on the current month. For example, the average onset time in the late spring months was earlier than the average onset time during the winter months, particularly December and January (not shown).

Table 2. A summary of statistical properties of the land-breeze onset times (hours after sunset) under various surface flow regimes during the non-convective season. The onset times are categorized based on the sea-breeze (SB) occurrence or absence, and surface synoptic flow according to mean sea level pressure charts.

October to May: SB during preceding afternoon							
Surface Synoptic Flow	*Median Onset Time*	*50% of Events*	*80% of Events*	*Min*	*Max*	*St. Dev.*	*Sample Size*
Offshore (NW/W/SW)	2.5	1.1 to 4.3	0.3 to 4.9	0.0	5.5	1.7	43
Onshore (NE/E/SE)	6.4	4.5 to 9.4	3.1 to 10.7	1.8	12.3	3.1	18
Shore-Parallel (S/N)	5.5	2.4 to 6.4	0.9 to 7.5	0.7	10.4	2.7	18
Light & Variable	4.8	3.8 to 6.1	3.3 to 7.5	1.9	8.0	1.8	18

October to May: No SB during preceding afternoon							
Surface Synoptic Flow	*Median Onset Time*	*50% of Events*	*80% of Events*	*Min*	*Max*	*St. Dev.*	*Sample Size*
Offshore (NW/W/SW)	3.1	2.6 to 3.4	0.9 to 4.3	0.2	4.4	1.3	12
Onshore (NE/E/SE)	7.0	5.2 to 9.3	3.2 to 11.4	2.7	13.1	2.9	53
Shore-Parallel (S/N)	5.5*	Sample size too small*	Sample size too small*	2.2	13.7	4.0*	7*
Light & Variable	6.4	3.4 to 7.5	2.7 to 8.7	2.5	9.2	2.5	11

*The percentile ranges were excluded for sample sizes less than 10. Use the standard deviation with caution for categories with such small sample sizes.

Guidance for Predicting Land-Breeze Direction/Movement

The frequency distributions of land-breeze directions versus surface-flow directions are shown in Figure 5. By comparing Figures 5a and b, it is evident that there are somewhat different distributions of favored land-breeze directions during the non-convective season versus the convective season. During the non-convective season, there are four favored relationships between the surface flow and land-breeze direction:

- NE or E surface flow yielding a NW land-breeze,

- SE surface flow yielding a SW land-breeze,

- SW surface flow yielding a SW land-breeze, and

- NW surface flow yielding a W land-breeze.

During the convective season, there are only two relationships between the surface flow and land-breeze directions:

- SE surface flow yielding a W or SW land-breeze, and

- SW or W surface flow yielding a SW land-breeze.

There were other wind-shift combinations that occurred during the seven-year climatology. However, the most favorable scenarios are listed above and are based on the distinct maxima seen in Figures 5a and b.

By decomposing the frequency diagrams into events that had a sea-breeze occurrence or absence during the preceding afternoon, we can see quite disparate distributions during the non-convective season (Figures 5c and e). When a sea breeze precedes the land breeze (Figure 5c), the surface flow is primarily from the SW, and secondarily from the W or NW, whereas the land-breeze typically comes from the SW or W direction. However, when a sea breeze does not precede the land breeze (Figure 5e), the surface flow is almost always from an onshore direction. The favored combinations in this scenario are SE flow with a SW land breeze, and NE to E flow with a NW land breeze.
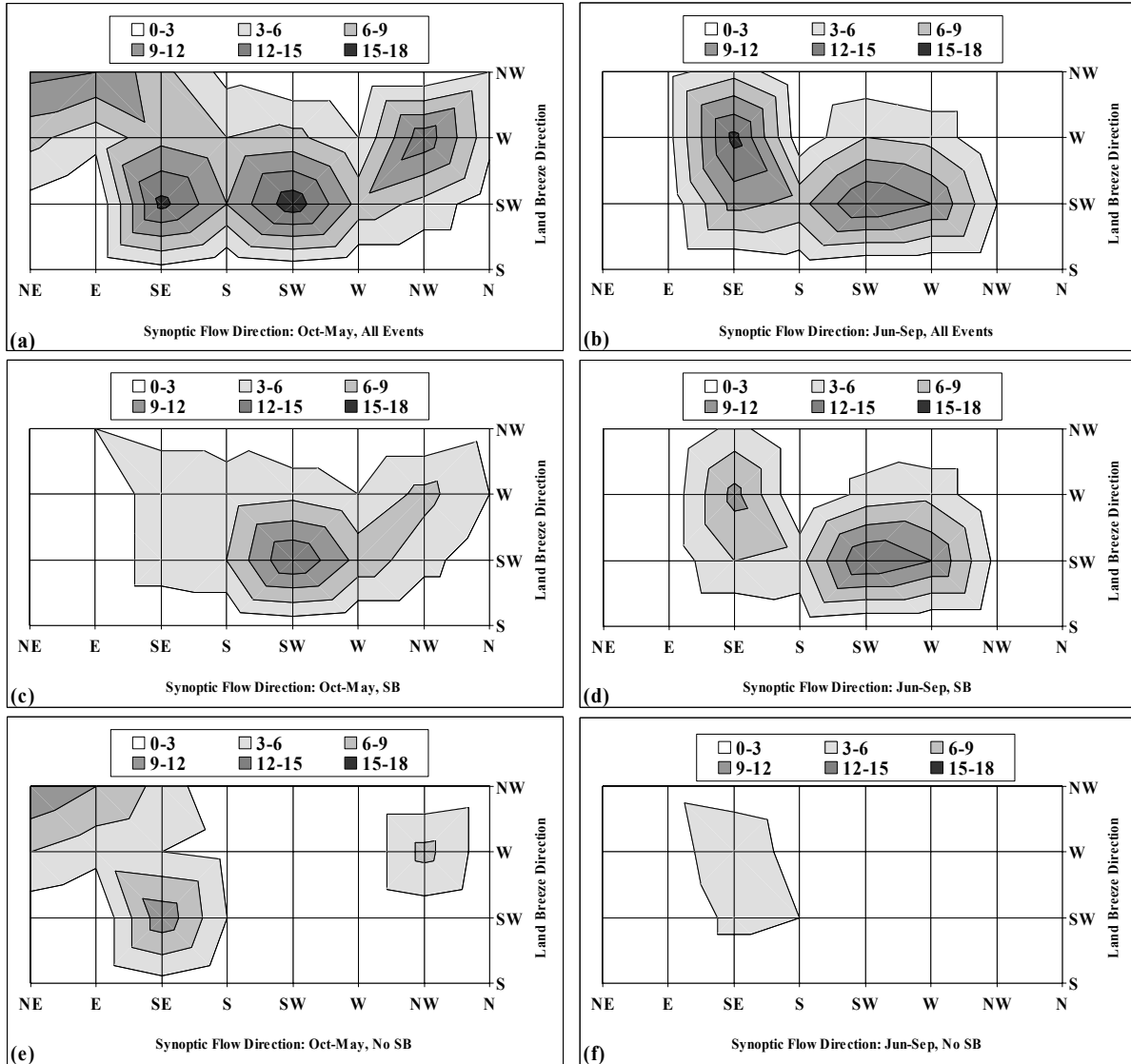
Figure 5. The frequency distributions of land-breeze directions from February 1995 to January 2002 as a function of the synoptic flow direction, based on a categorization of events into minimal convective (October to May) versus peak convective months (June to September), and events with and without a preceding sea breeze (SB). All events are shown for the months of (a) October to May, and (b) June to September. Events preceded by a sea breeze are shown for (c) October to May, and (d) June to September. Events without a preceding sea breeze are shown for (e) October to May, and (f) June to September.

These forecast products are intended to be stand-alone guidance that forecasters can use throughout the year. The flowcharts, tables, and diagrams will be delivered to the 45 WS once finalized and approved. For more information on this work, contact Mr. Case at 321-853-8264 or case.jonathan@ensco.com.

IMPROVED ANVIL FORECASTING PHASE III (DR. SHORT AND MR. WHEELER)

The 45 WS Launch Weather Officers (LWOs) have identified anvil forecasting as one of their most challenging tasks when attempting to predict the probability of an LCC violation due to the threat of natural and triggered lightning. SMG forecasters have reiterated this difficulty when evaluating Space Shuttle FRs. Phase II of this task resulted in the operational implementation of an observations-based nowcasting tool, based on the high correlation between anvil propagation characteristics and the observed wind speed/direction in the anvil layer, between 300 and 150 mb (Short and Wheeler 2002a). The Anvil Threat Sector tool graphically overlays an anvil threat corridor sector for a user-selected station on a weather satellite image. The goals of Phase III are to build upon the results of Phase II by enhancing the anvil threat corridor sector tool with the capability to use model forecast winds for depiction of potential anvil lengths and orientations over the KSC/CCAFS area with lead times from 1 to 72 hours.

The anvil threat sector tool developed in Phase III uses an average of the upper-level winds between 300 and 150mb from either the most current ETA or Medium Range Forecast (MRF) model point data to plot its threat sector, depending on the forecast verification time. The forecast anvil threat sector can be displayed every hour from 1 - 60 hours using the Eta point data and at 72 hours using wind data from the MRF point data.

Figure 6 shows an example of the forecast Anvil Threat Sector. Input from the user centered the plot on Space Launch Complex 37 (SLC-37) and specified a forecast of 1 hour using upper-level winds from the Eta model point data. On the top right is a legend that shows what model was used, the Julian date and UTC time of the model input, forecast wind direction and speed, and the center point. A copy of the current version has been sent to SMG for their review and it has also been shown to several 45 WS LWOs for their comments.
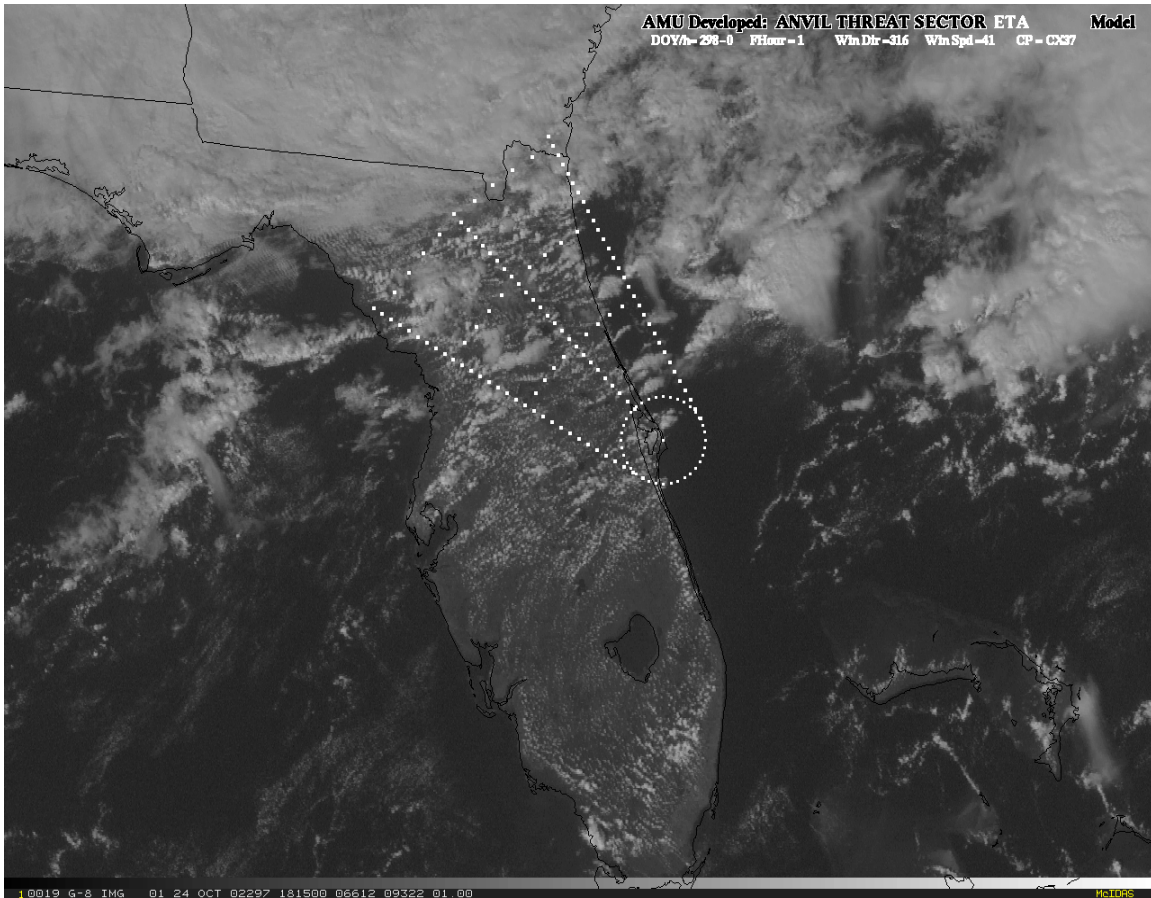

Figure 6. Example of an anvil threat sector using the Phase III anvil forecast plotting utility. The white dots highlight the anvil threat sector using SLC-37 as the center point, and a 1-hour forecast using upper-level winds from the Eta model point data.

For more information on this work, contact Dr. Short at 321-853-8105 or short.david@ensco.com, or Mr. Wheeler at 321-853-8205 or wheeler.mark@ensco.com.

EXTEND STATISTICAL FORECAST GUIDANCE FOR THE SLF TOWERS (MS. LAMBERT)

As stated in the Statistical Short-Range Forecast Tools section of this report, the peak winds near the surface are an important forecast element for both the Space Shuttle and ELV programs. As defined in the LCC and the Shuttle FRs, each vehicle has certain peak wind thresholds that cannot be exceeded in order to ensure the safety of that vehicle during launch and landing operations. The 45 WS and the SMG indicate that peak winds are a challenging parameter to forecast. In Phase I of this task, climatologies and distributions of the 5-minute average and peak winds were created for all towers used in evaluating LCCs and FRs (see Table 1). However, SMG uses a 10-minute peak as the standard for determining and verifying wind speed FRs. The goal of this phase of the task is to re-calculate the distributions and resulting probabilities of exceeding peak-wind thresholds using a 10- instead of 5-minute peak for the SLF towers for all months. A tool that can be used on a personal computer (PC) will also be developed to display the desired information quickly and easily.

Climatologies and Distributions

The first step in this task was to determine the 10-minute peak for each 5-minute average wind in the data set. Ms. Lambert developed an algorithm in S-PLUS that compared a peak wind speed with its corresponding value five minutes earlier. The larger of the two was chosen as the value for the associated 5-minute average wind speed. Ms. Lambert then computed the same hourly, directional, and hour by direction climatologies as in Phase I of this task. The 10-minute peak wind speed means and standard deviations were only slightly higher than the 5-minute peak speed means calculated in Phase I. Microsoft$^®$ Excel Pivot Charts of the climatologies were created by Ms. Lambert as an interim product for SMG until the PC-based tool can be developed.

After creating the climatologies, Ms. Lambert created the empirical probability density functions (PDFs) of 10-minute peak wind speed for every 1 knot in the 5-min average wind speeds. These PDFs show the forecasters the probability of meeting or exceeding a specific peak speed given an average wind speed based on past observations in the 7-year database. Ms. Lambert then conducted tests to determine the theoretical distribution that provided a best-fit to the empirical PDFs. This was done for two reasons as discussed in Wilks (1995): 1) to interpolate over the variations in empirical PDfs due to possible under-sampling of a specific peak gust, and 2) to estimate probabilities of 10-minute peak gusts associated with average wind speeds outside the range of observed values in the data set. In Phase I, the 5-minute peak speed PDFs were found to be Weibull distributed. However, the Kolmogorov-Smirnov goodness-of-fit test (Wilks 1995) and graphical displays indicated overwhelmingly that the 10-minute peak speed PDFs were gamma distributed.

Wilks (1995) describes both the gamma and Weibull distributions as asymmetrical with a physical limit (e.g. 0) on the left side. However, it also states that the Weibull distribution is most often used to model variations in wind speeds, while the gamma distribution is most often used to represent precipitation data. A cursory literature search revealed little support for use of the gamma distribution with wind speeds, but Ms. Lambert will conduct a more thorough search in the next quarter.

For more information on this work, contact Ms. Lambert at 321-853-8130 or lambert.winifred@ensco.com.

INSTRUMENTATION AND MEASUREMENT

I&M AND RSA SUPPORT (DR. MANOBIANCO AND MR. WHEELER)

Mr. Wheeler met with several Lockheed Martin personnel to review and finalize the RSA AMU equipment, console and floor plans. The new tentative installation date of the equipment is February 2003.

Table 3. AMU hours used in support of the I&M and RSA task in the fourth quarter of FY 2002 and total hours since July 1996.	
Quarterly Task Support (hours)	*Total Task Support (hours)*
14	348.5

EXTEND AMPS MOISTURE PROFILES (DR. SHORT AND MR. WHEELER)

The 45 WS utilizes vertical profiles of humidity and temperature from balloon-borne radiosonde observations (RAOBs) to assess atmospheric stability and the potential for thunderstorm activity. Operational RAOBs from the Meteorological Sounding System (MSS) will be replaced by the Low Resolution Flight Element (LRFE) of the Automated Meteorological Profiling System (AMPS) at the balloon facility (XMR) on CCAFS in the near future. Testing of the AMPS LRFE (hereafter AMPS) and earlier comparisons with MSS revealed significant differences in relative humidity (RH) between the two systems (Leahy 2002; Short and Wheeler 2002b). Because local experience and thunderstorm forecast rules of thumb are based on a long history of stability indices computed from MSS RAOBs, and because the vertical profile of RH is a sensitive indicator of atmospheric stability, it is important that forecasters become familiar with any changes in humidity data that accompany the transition to AMPS RAOBs. The AMU was tasked to examine the RH differences in detail to evaluate the impact of the humidity differences on the diagnosis of atmospheric stability and thunderstorm indices.

A special data collection campaign was conducted at XMR during July and August 2002, resulting in 20 pairs of humidity and temperature profiles from balloon flights that carried both AMPS and MSS sensors. This warm-season campaign was designed to supplement the cool-season campaign that had been carried out earlier in the year and reported in Short and Wheeler (2002b). For the present task extension, Dr Short and Mr. Wheeler are performing a study of the 20 warm-season dual-sensor profiles to determine if the humidity differences seen during the cool-season campaign also occurred in the warm-season campaign. Dr. Short will also evaluate the impact of the observed humidity differences on thunderstorm forecasting indices used operationally by the 45 WS, SMG, and the National Weather Service Office at Melbourne, FL (NWS MLB).

Background

Dr. Short and Mr. Wheeler conducted an objective comparison of 20 dual-sensor profiles taken at XMR during the months of January, February and April 2002. Their analysis of RH differences from the cool-season dual-sensor profiles showed a systematic bias pattern between the current operational system, MSS, and its planned replacement system, AMPS. The AMPS RH averaged 5% greater than the MSS RH when the MSS RH was above 50%. Conversely, for MSS values lower than about 30%, the AMPS RH averaged about 10% lower. The impact of the systematic RH differences on stability indices made the atmosphere appear less stable when diagnosed with the AMPS RH profile. Stability indices and atmospheric parameters analyzed for each of the 20 cool-season dual-sensor profiles were the Showalter Index, the Lifted Index, the K-Index, Total Totals, Convective Available Potential Energy (CAPE), precipitable water, and the Microburst Day Potential Index (MDPI).

Dr. Short and Mr. Wheeler also made an estimate of the impact of the RH difference pattern on warm-season stability indices computed from climatological warm-season profiles. Typical values of the K-Index and Total Totals were about 1 to 2 units higher. Typical values of the Showalter Index and the Lifted Index were about 1 unit lower. CAPE was enhanced by about 25%, precipitable water was 5% higher and the MDPI was enhanced by 10 to 15%. Dr. Short and Mr. Wheeler made interim operational recommendations for adjusting stability indices and atmospheric parameters on the basis of these estimates. The recommendations have been taken under advisement by the 45 WS, pending an analysis of the warm-season dual sensor profiles.

Warm-Season Dual-Sensor Profiles

Table 4 lists the AMU inventory of XMR dual-sensor profiles obtained from Computer Sciences Raytheon (CSR) from the warm-season campaign. Dr. Short implemented a subjective quality control process to identify outliers and significant overall discrepancies in either the AMPS or MSS profiles.

Table 4. List of dates and times of AMPS/MSS dual-sensor profiles from XMR used in the analysis of data from the 2002 warm season.			
Number	*Month*	*Day*	*Time (UTC)*
1	July	19	1500
2	July	22	1500
3	July	23	1510
4	July	25	1500
5	July	26	1500
6	July	29	1500
7	July	30	1500
8	July	31	1500
9	August	1	1500
10	August	2	1500
11	August	3	1500
12	August	4	1500
13	August	5	1500
14	August	6	1500
15	August	7	1500
16	August	8	1500
17	August	9	1500
18	August	10	1500
19	August	11	1500
20	August	14	1500

Each dual-sensor profile listed in Table 4 was obtained from MSS and AMPS sensor packages suspended below a weather balloon carrying them aloft at an ascent rate of approximately 1000 ft per minute. The MSS sensor package was 35 ft above the AMPS, leading it by about 2 seconds as the balloon ascended. The time difference did not have an impact on this or previous studies.

Under normal operations the MSS uses a dual-tone radio-transponder/radar-tracking system to determine range, azimuth and elevation information and to infer altitude, wind speed and wind direction. However, for dual-sensor flights the MSS ranging signal was turned off in order to avoid interference with the AMPS ground equipment. As a result the MSS data stream did not have its normal radar telemetry information and the MSS files contained only

time, temperature and humidity measurements every six seconds, with no height, pressure or wind data.

AMPS employs global positioning technology to determine altitude, latitude and longitude, from which wind speed and direction are estimated. Pressure for the AMPS profile is calculated from the altitude, pressure, temperature and humidity. Time altitude, pressure, temperature and humidity are reported every second in the raw AMPS data files.

AMU Analysis of MSS vs. AMPS Humidity Differences

Profiles of MSS and AMPS RH were merged by matching times within each sounding. Numerous profiles required a minor time adjustment to improve the match-up between the RH profiles reported by the two instruments. The 20 dual-sensor profiles were then filtered by excluding levels with pressures less than 100 mb and by excluding data pairs where the temperature difference between the two sensors was more than 1°C. The resulting data is confined largely to the troposphere, where atmospheric convection originates, and emphasizes differences in RH between the two systems. The quality control procedure resulted in 9036 pairs of AMPS/MMS RH readings for analysis.

Figure 7 shows average MSS RH versus average AMPS RH for 10% intervals of MSS RH from 10% to 100%. A fourth order polynomial fit to the average data points is shown as a thick solid line. The thin dashed line indicates the results of the cool-season comparison. The regular solid line indicates a 1:1 ratio between the AMPS and MSS RH values. The warm season profiles show the same pattern of RH differences found in the cool-season profiles with one exception. In the range of RH values from 50% to 80% the warm season profiles show better agreement between the two sensors. It can be expected that the warm-season profiles will show slightly smaller differences in stability indices, however the AMPS would still be expected to indicate a less stable atmosphere than the MSS.
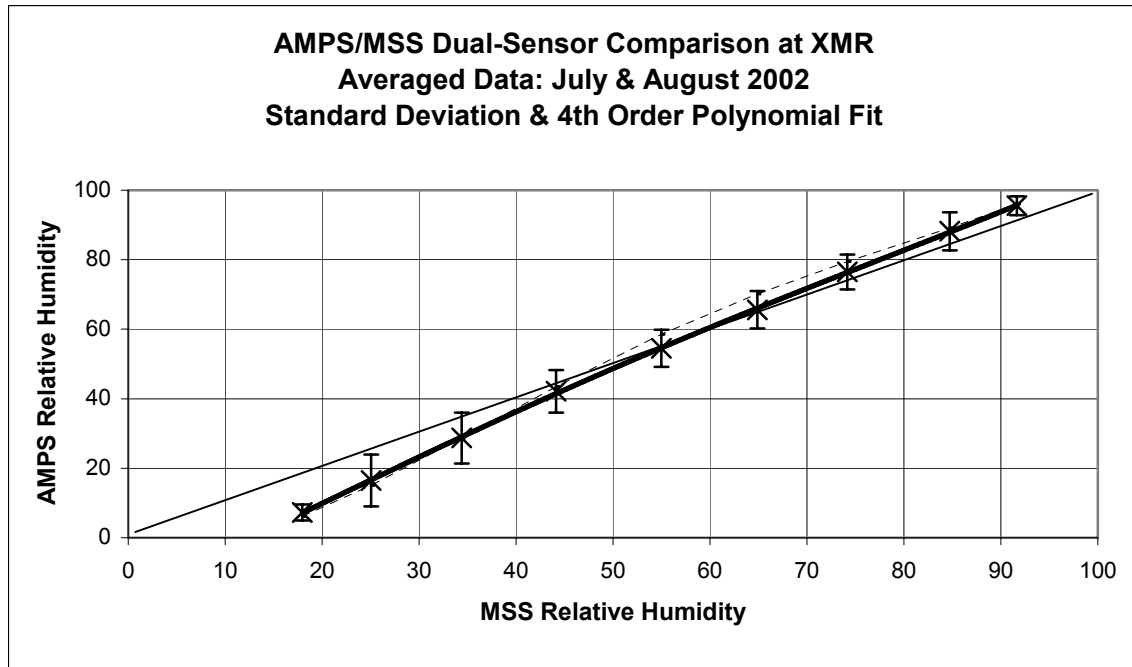

Figure 7. Average MSS RH versus average APMS RH for 10% intervals of MSS RH from 10% to 100%. The regular solid line indicates a 1:1 ratio between the AMPS and MSS RH values. A fourth-order polynomial fit to the 9 average data points is shown by the heavy solid line and has the equation: $Y = -16.202 + 1.2270 \, X + 0.0061737 \, X^2 - 0.00012755 \, X^3 + 0.0000006487 \, X^4$. Vertical bars represent the standard deviations of RH values within each 10% interval. The thin dashed line represents the MSS versus AMPS curve derived from data taken during January, February, and April 2002.

Figure 8 shows the vertical profiles of average RH from both sensors. The AMPS pressure was used for both profiles. At pressures greater than 700 mb the AMPS shows higher RH values reaching a difference of approximately 5% at 1000 mb. At pressures less than 700 mb the AMPS shows RH values lower than the MSS, reaching a difference of 10% at 200 mb.

The RH profiles shown in Figure 8 indicate increased low-level humidity and decreased upper level humidity from the AMPS compared to the MSS. The difference in the vertical profile of RH would increase the instability of the atmosphere, as diagnosed from AMPS soundings. This result is consistent with the previous analysis of dual-sensor profiles from the cool-season. A quantitative analysis of stability indices will be made during the next quarter.
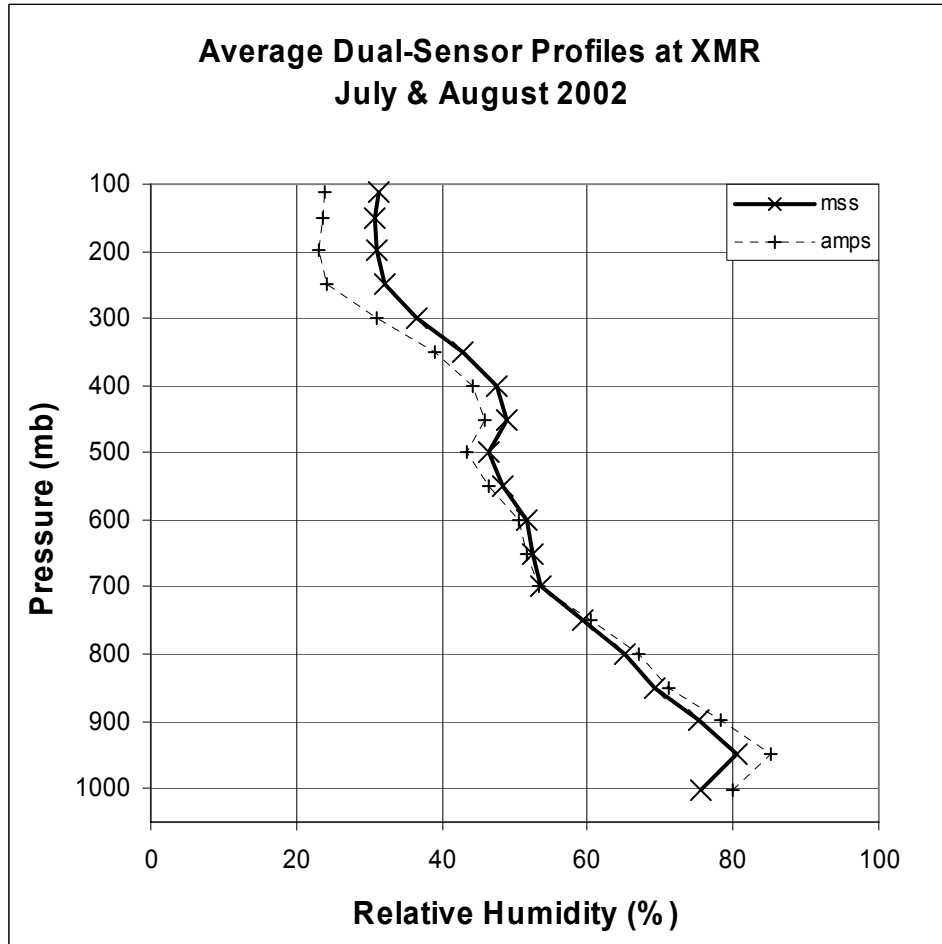

Figure 8. Vertical profiles of average relative humidity from the MSS (solid) and AMPS (dashed) sensors for twenty dual-sensor ascents taken in July and August 2002.

For more information on this work, contact Dr. Short at 321-853-8105 or short.david@ensco.com, or Mr. Wheeler at 321-853-8205 or wheeler.mark@ensco.com.

MINISODAR EVALUATION (DR. SHORT AND MR. WHEELER)

The Doppler miniSODAR™ System (DmSS) is an acoustic wind profiler from AeroVironment, Inc., that provides vertical profiles of wind speed and direction with high temporal and spatial resolution. The DmSS in this evaluation is a model 4000 system, configured to provide wind estimates every minute at 23 height levels from 15 to 125 m, or 49.2 to 410.1 ft, every 5 m, or16.4 ft,. The DmSS is a phased array system with 32 speaker elements that are used to form 3 beams for measuring orthogonal components of the wind field, 2 horizontal and 1 vertical. The Boeing Company installed a DmSS at SLC-37 as a substitute for a tall wind tower. It will be used to evaluate the launch pad winds for the new Evolved ELV during ground operations and to evaluate LCC during launch operations. In order to make critical GO/NO GO launch decisions, the 45 WS LWOs and forecasters need to know the quality and reliability of DmSS data.

Sensor Locations and Siting Issues

The AMU was tasked to perform an objective comparison between the DmSS wind observations near SLC-37 and those from the nearest tall ($\geq$ 204 ft) wind tower. The tall wind tower that is nearest to SLC-37 is 0006. Tower 0108 with a height of 54 ft is closer to the DmSS than tower 0006, as shown in Figure 9, and will also be used in the comparison study. Mr. Wheeler began collection of data from these towers and the DmSS in August 2002.
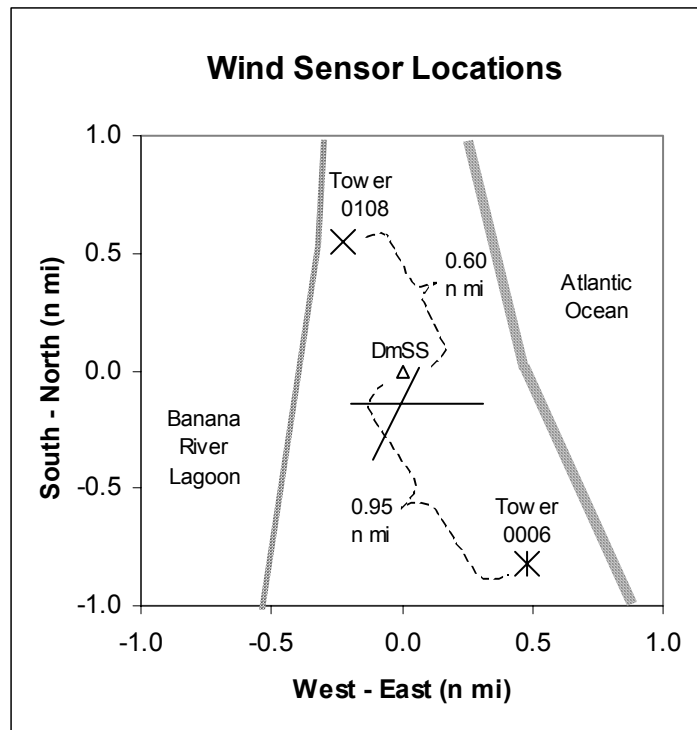

Figure 9. Locations of Towers 0006, 0108 and the DmSS, with approximate geographic features. The distance between tower 0006 and the DmSS is 0.95 n mi. Tower 0108 is closer (0.60 n mi), but is only 54 ft tall. The intersecting solid lines near the DmSS site indicate nearby roads.

The distance between the DmSS and wind towers will affect the nature of comparisons that can be made. Turbulent variations of wind speed and direction will result in an increase in errors between sensor readings as the distance between the sensors increases. However, the error can be expected to decrease as the time averaging of the data increases. The theoretical error (%) for a comparison under ideal conditions has been modeled by the following equation (Crescenti 1997):

$$\varepsilon^2 = \frac{2}{T}\frac{\sigma_U^2}{U^2}\int_0^\infty R(t)\,dt \tag{1}$$

where T is the averaging time-scale for the data, U is the prevailing wind speed along the line between the sensors, σ_u is the standard deviation of wind speed and R(t) is the autocorrelation function of the wind speed. The integral can be represented by a second time-scale equal to d/U, where d is the separation distance. The ratio σ_u/U has been found to be approximately 0.224 in previous studies (Wyngaard 1973).

Figure 10 shows the expected error as a function of separation distance for a wind velocity of 10 kts and data averaging times of 5, 10, 20 and 40 minutes. For example, at a separation distance of 0.6 n mi with a wind velocity of 10 kts, an averaging time of 40 minutes would be expected to result in comparison errors of +/- 1 kt (10%). A 5-minute averaging time under the same conditions would result in comparison errors of +/- 2.7 kts (27%).
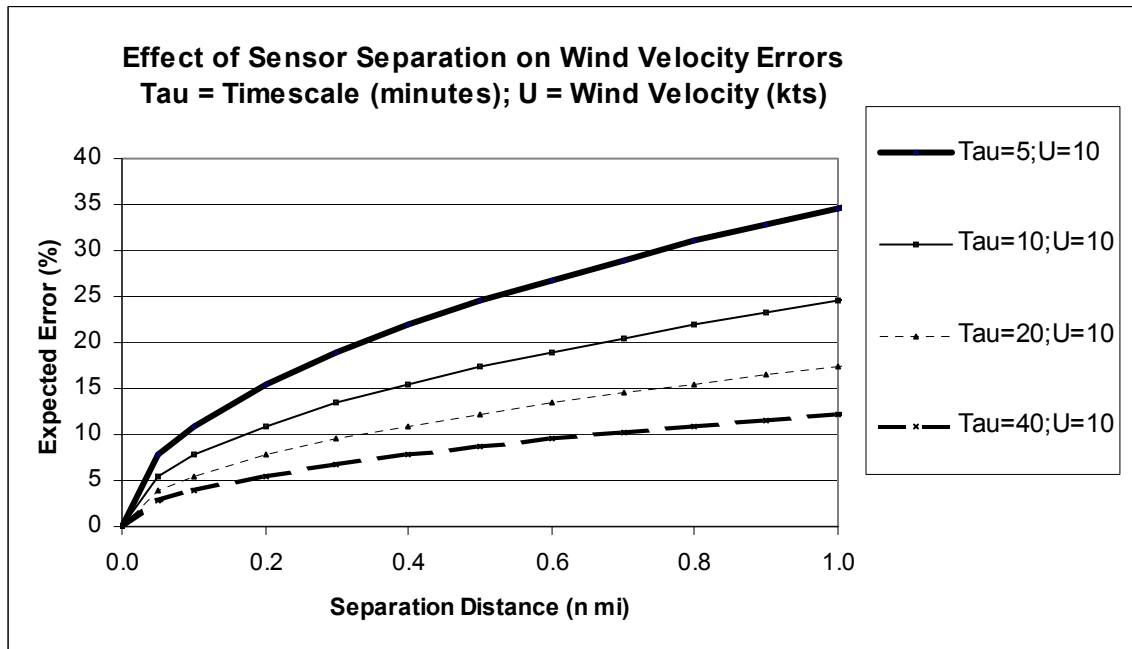

Figure 10. Expected errors as a function of separation distance for wind velocity comparisons under ideal conditions.

Figure 11 shows the DmSS as it was installed by Boeing on a concrete pad near SLC-37. The view direction is toward the SW. General guidelines from the World Meteorological Organization (WMO) for the siting of wind sensors are to place them at a distance equal to or greater than ten times the height of the nearest obstruction (WMO 1983). It appears that the wind field at the present DmSS site could be influenced by the nearest building, especially when the wind blows from the SSW. An additional factor that could affect data quality would be traffic along the 2-lane road that runs parallel to the front of the building, about 60 ft to the left. It is possible that the DmSS signal could be influenced by acoustic noise or reflected sound waves from vehicles traveling along the road, which has a posted speed limit of 35 mph, or 30.4 kts. One possible solution for minimizing such effects would be to add acoustic baffles to the DmSS. Routine maintenance of the DmSS would also be advised to assure that it is fully operational. The loss of a speaker element would compromise the beam form and increase the probability of unwanted contamination of acoustic signals.

Figure 11.   Photograph of DmSS site and nearby building. The DmSS and building are separated by about 40 ft. A 2-lane road runs parallel to the front of the building approximately 60 ft to the left.

The DmSS site includes a sonic anemometer on a 33 ft (10 m) pole that is behind the building and partially obscured from view by the pole in the foreground. Sonic anemometer data is integrated into the DmSS data stream and could be included in the comparison study.

Data Structures

The DmSS data is recorded on a PC system in the Range Weather Operations (RWO) facility within the Range Operations Control Center (ROCC). Every minute the DmSS reports wind speed and direction at each of 23 height levels. In addition, a gust speed and direction, a vertical wind velocity and numerous measures of system performance such as signal intensity and signal-to-noise ratio are reported. Missing data are reported as 9999 or 99.99 depending on the variable. The AMU has obtained permission from the 45 WS and Boeing to download DmSS data from the RWO PC on a non-interference basis.

The tower data is averaged over 5-minute intervals with the average speed, average direction, peak 1-second speed and direction archived for analysis. Variability of the wind direction is also reported in addition to temperature, dew point and relative humidity at selected levels. Missing data are not reported. Quality control (QC) software is available for removing outliers in the data based on climatological statistics and vertical consistency checks.

Preliminary Data Examples

The following preliminary examples of time-coincident DmSS and tower data serve to illustrate several expected meteorological characteristics and one clear signature of anomalous DmSS data. Figure 12 shows a 6-hour time series from 28 August 2002 of wind direction from the DmSS and Towers 0006 and 0108. The passage of a sea breeze is clearly evident around 1630 UTC. Wind directions shift from SW to ESE with the shift occurring first at Tower 0006, then at the DmSS site and then at Tower 0108. This delayed timing is consistent with a sea breeze moving inland. Directional variations are evident from all three sensors before, during and after the sea breeze passage. The pattern of variation is too complex to interpret as a simple propagating phenomena. This lack of coherence at short time-scales is typical of the turbulent wind field near the earth's surface.
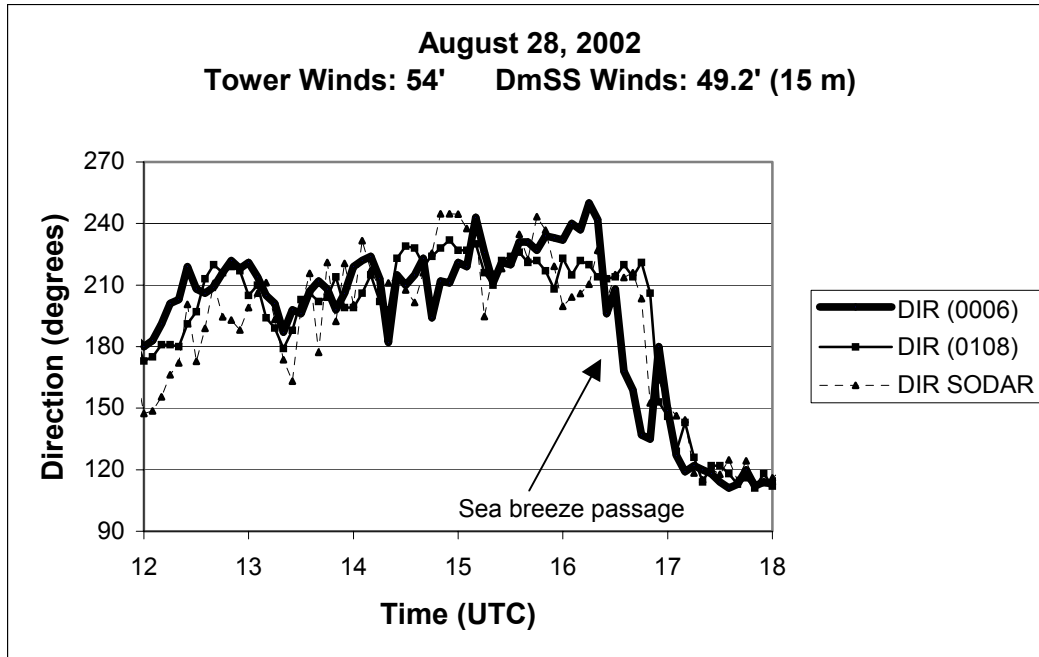
Figure 12. A 6-hour time series of wind direction from the 54 ft level on Towers 0006 (solid thick line) and 0108 (solid thin line), and the 49.2 ft (15 m) level from the DmSS (dashed thin line). A sea breeze passage is indicated around 1630 UTC.

Figure 13 shows a 6-hour time series of wind speed at 162 ft from Tower 0006 and 164 ft (50 m) from the DmSS. A sea breeze passage is not evident in the wind speed, however the DmSS and tower wind speeds are reasonably consistent for the first 4.5 hours with minor incoherent variations as seen in the wind direction (Figure 12). Anomalous DmSS wind speeds of about 30 kts were seen just before 1700 and 1800 UTC. The anomalous wind speeds are consistent with possible acoustic contamination from vehicular traffic along the nearby road. Wind directions associated with these peaks were from the WNW (about 300°). Such anomalous data would not be expected from a well-maintained instrument in an acoustically quiet environment.

August 28, 2002
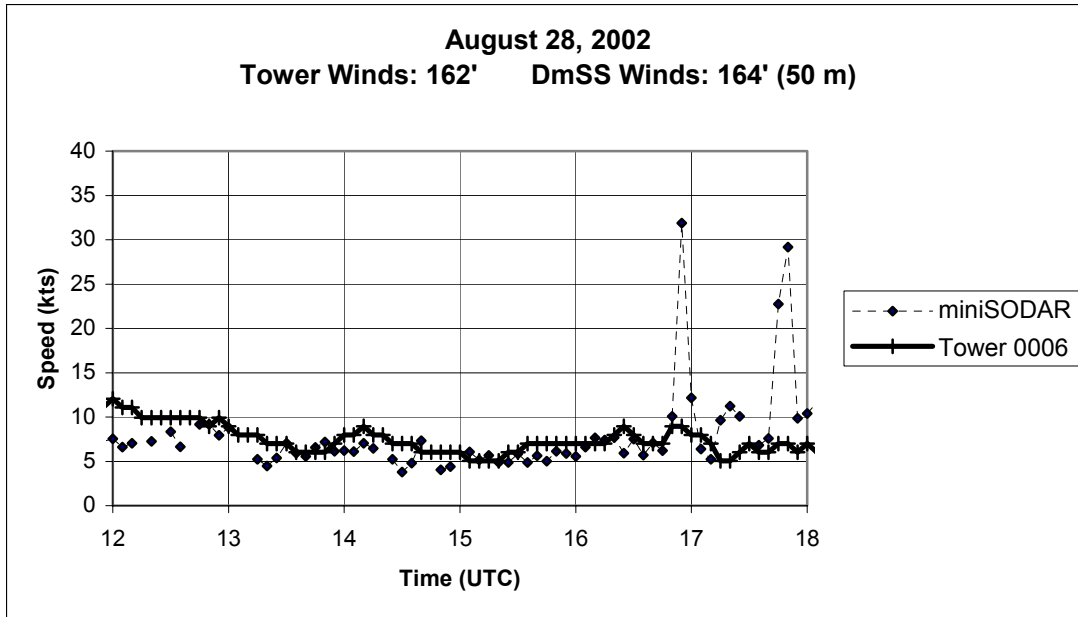## Tower Winds: 162'   DmSS Winds: 164' (50 m)

Figure 13.   A 6-hour time series of wind speed from 162 ft on Tower 0006 and 164 ft (50 m) from the DmSS. High speed outliers in the DmSS data near 1700 and 1800 UTC are not consistent with the prevailing meteorological conditions.

The DmSS had not undergone any routine maintenance since its installation several months earlier. Maintenance by the vendor had been scheduled for early October at the time of this writing.

For more information on this work, contact Dr. Short at 321-853-8105 or short.david@ensco.com, or Mr. Wheeler at 321-853-8205 or wheeler.mark@ensco.com.

MESOSCALE MODELING

LOCAL DATA INTEGRATION SYSTEM OPTIMIZATION AND TRAINING EXTENSION (MR. CASE)

Both SMG and NWS MLB are running a real-time version of the Advanced Regional Prediction System (ARPS) Data Analysis System (ADAS) to integrate a wide-variety of national- and local-scale observational data. While the analyses have become more robust through the inclusion of additional local data sets as well as the modification of several adaptable parameters, further improvements are desired prior to configuring and initializing the ARPS model with ADAS analyses in future AMU tasks. In addition, limited training would facilitate the transfer of the ARPS/ADAS software configuration and maintenance responsibilities to the NWS MLB and SMG. As a result, the AMU is tasked to improve the real-time data ingest by improving the background fields, expanding the analysis domain, including additional data sets, and modifying the ingestion of selected data sets. Finally, the AMU will provide limited training to NWS MLB and SMG forecasters regarding the maintenance of data-ingest programs and adjustments to the local ADAS configuration.

Mr. Case met with NWS MLB representatives to discuss the prioritization of several items for this task. The NWS MLB expressed interest to update the background fields first, then expand the analysis domain in preparation for the future ARPS task, and finally incorporate new data sets and re-format existing observational data. Currently, the real-time configuration of the ADAS at NWS MLB uses Rapid Update Cycle (RUC) forecasts interpolated to the old 40-km grid, and acquires these data once every 3 hours. In addition, RUC data are time-interpolated between the 3- and 6-hour forecast grids to serve as background fields for ADAS. Mr. Case acquired existing routines from SMG that obtain RUC 1- to 3-hour forecasts every hour from the full-resolution 20-km grids. He will assist the NWS MLB in the acquisition and processing of these new RUC data to mimic SMG's current configuration.

For more information on this work, contact Mr. Case at 321-853-8264 or case.jonathan@ensco.com.

VERIFICATION OF NUMERICAL WEATHER PREDICTION MODELS (DR. MANOBIANCO AND MR. CASE)

This project is an option-hours task funded by KSC under the Center Director's Discretionary Fund. It is a joint effort between the KSC Engineering Support Contractor, Dynacs, Inc., and the AMU. A key to improving mesoscale numerical weather prediction (NWP) models is the ability to evaluate the performance of high-resolution model configurations. Traditional objective evaluation methodologies developed for large-scale models cannot verify phenomenological forecasts from mesoscale models, and subjective manual alternatives are lengthy and expensive. New objective quantitative techniques are required for evaluating high-resolution, mesoscale NWP models. Therefore, in coordination with personnel from Dynacs, Inc., the AMU was tasked to develop advanced techniques for the objective evaluation of mesoscale NWP models currently employed or under development for Range use. Archived Regional Atmospheric Modeling System (RAMS) forecasts and KSC/CCAFS wind-tower observations will be used to develop the objective verification algorithms for the sea-breeze phenomenon. The verification of sea breezes was chosen because this phenomenon is predicted fairly well by RAMS and the sea-breeze boundary is often nearly linear and narrow in width, making the geometry simple.

In this past quarter, the Dr. Manobianco and Mr. Case met periodically with Dynacs representatives and the principle investigator, Dr. Merceret, to discuss progress on the Dynacs objective software and technique, named Contour Error Map (CEM). To help evaluate CEM, Mr. Case compiled a spreadsheet of his subjective determination of the daily observed sea-breeze occurrence and onset time during the month of July 2000 (the working data set). This spreadsheet was used by Dynacs to help identify the successes and shortfalls of the CEM software with the working data set. Furthermore, all participants met to examine and discuss the output of CEM in comparison to the meteorological and RAMS forecast fields.

To improve the robustness and accuracy of CEM results, all participants agreed that higher temporal resolution data are required, in addition to data for all 24 hours of each day. Up to this point in the project, Dynacs had been using hourly forecast output from RAMS for comparison to observed fields in CEM only during the daylight hours of 1200 UTC to 2300 UTC. To improve the quality of the verification technique, 5-minute observed and forecast data are desired for each day. In addition, Dynacs determined that a filtering technique would be helpful to isolate the sea-breeze signal from other signals in the time series data; however, filtering requires continuous temporal data in order to apply the technique(s) adequately. Therefore, the Mr Case processed observed wind-tower data every 5 minutes at all times of every day during July 2000, and provided these data to Dynacs. In addition, Mr. Case provided Dynacs with all available hourly RAMS forecasts for July.

Another issue raised by Mr. Case was that many days during July 2000 were unfavorable for sea-breeze verification due to the synoptic conditions and frequent precipitation contamination. Furthermore, several days had many missing wind-tower observations, rendering the verification suspect due to limited data availability. Contrary to July, August 2000 had very little precipitation, and the archived wind-tower data were much more complete. As a result, the Mr. Case processed all data for August in the same manner described above.

Finally, to provide Dynacs with 5-minute forecast output for both July and August 2000, the AMU is required to re-run RAMS forecasts in order to generate archived output at this temporal frequency. To achieve this forecast output, Mr. Dianic modified several scripts so that RAMS will re-run all forecasts and generate output every 5 minutes. These forecasts are currently being run on an AMU workstation, which is capable of completing two forecasts per day. As of mid-October, about half of the 1200 UTC RAMS forecasts were completed, and it is estimated that all 1200 UTC forecasts will be completed by early November. Mr. Case is providing these data to Dynacs as they become available.

For more information on this work, contact Mr. Case at 321-853-8264 or case.jonathan@ensco.com.

AMU CHIEF'S TECHNICAL ACTIVITIES (DR. MERCERET)

Dr. Merceret and Ms. Ward completed manual quality control of the 1999 - 2001 data from the 915 MHz profilers, and presented a briefing at the Range Operations Control Center on the availability and quality of the 915 MHz profiler data. Dr. Merceret began meteorological analysis of 23 selected days that exemplify the ability of the boundary layer profilers to identify and describe phenomena such as fronts, low-level jets, inversions, and sea or land breezes. He also presented an analysis of the 24 June 2001 tornadic storm case to the Airborne Field Mill (Lightning Launch Commit Criteria) science team on 19 September.

AMU OPERATIONS

Mr. Wheeler worked with NASA Procurement on the delivery of previously ordered software. This completed the 2001 FY procurement of AMU equipment and software from NASA and outside vendors. An updated version of the weather display software (McIDAS 2002) was installed and configured on one of the HP UNIX systems.

Mr. Case attended the AMS 19th Conference on Weather Analysis and Forecasting in San Antonio, TX, where he presented results from the Land Breeze Forecasting task.

REFERENCES

Crescenti, G. H., 1997: A look back at two decades of Doppler SODAR comparison studies. *Bull. Amer. Meteor. Soc.*, **78**, 651-673.

Hsu, S. A., 2001: Spatial variations in gust factor across the coastal zone during Hurricane Opal in 1995. *National Weather Digest,* **25 Nos. 1 and 2**, 21-23.

Insightful Corporation, 2000: *S-PLUS® 6 User's Guide*, Insightful Corp., Seattle, WA, 470 pp.

Leahy, F., 2002: Analysis of the Automated Meteorological Profiling System Low Resolution Flight Element Thermodynamic data. Raytheon ITSS Memorandum to Stewart Deaton, NASA/MSFC/ED44, May 15 2002, 41 pp.

McVehil, G. E. and H. G. Camnitz, 1969: Ground Wind Characteristics at Kennedy Space Center. NASA Contractor Report CR-1418, Kennedy Space Center, FL, 102 pp.

National Aeronautics and Space Administration, 2000: Terrestrial Environment (Climatic) Criteria Handbook for use in Aerospace Vehicle Development. NASA-HDBK-1001, Section 2, 142 pp. [Available online at http://standards.nasa.gov].

Short, D. A., and M. M. Wheeler, 2002a: Improved Anvil Forecasting: Phase II Final Report. NASA Contractor Report CR-2002-211170, Kennedy Space Center, FL, 19 pp. [Available from ENSCO, Inc., 1980 N. Atlantic Ave., Suite 230, Cocoa Beach, FL, 32931.]

Short, D. A., and M. M. Wheeler: 2002b: AMPS Moisture Profiles. AMU Memorandum, July 2002, 16 pp. [Available from ENSCO, Inc., 1980 N. Atlantic Ave., Suite 230, Cocoa Beach, FL, 32931.]

Wilks, D. S., 1995: *Statistical Methods in the Atmospheric Sciences*. Academic Press, Inc., San Diego, CA, 467 pp.

WMO, 1983: Guide to Meteorological Instruments and Methods of Observation. World Meteorological Organization No. 8, 5th edition, Geneva, Switzerland.

Wyngaard, J. C., 1973: On surface-layer turbulence. Workshop on Micrometeorology, D. A. Haugen, Ed., Amer. Meteor. Soc., 101–149.

List of Acronyms

30 SW	30th Space Wing
30 WS	30th Weather Squadron
45 LG	45th Logistics Group
45 OG	45th Operations Group
45 SW	45th Space Wing
45 SW/SE	45th Space Wing/Range Safety
45 WS	45th Weather Squadron
ADAS	ARPS Data Analysis System
AFSPC	Air Force Space Command
AFWA	Air Force Weather Agency
AMPS	Automated Meteorological Profiling System
AMU	Applied Meteorology Unit
ARPS	Advanced Regional Prediction System
CAPE	Convective Available Potential Energy
CCAFS	Cape Canaveral Air Force Station
CEM	Contour Error Map
CSR	Computer Sciences Raytheon
DmSS	Doppler miniSODAR
ELV	Expendable Launch Vehicle
FR	Flight Rules
FSL	Forecast Systems Laboratory
FSU	Florida State University
FY	Fiscal Year
GF	Gust Factor
ITSS	Information Technology and Scientific Services
JSC	Johnson Space Center
KSC	Kennedy Space Center
LCC	Launch Commit Criteria
LDIS	Local Data Integration System
LRFE	Low Resolution Flight Element
LWO	Launch Weather Officer
MDPI	Microburst Day Potential Index
MRF	Medium Range Forecast
MSFC	Marshall Space Flight Center
MSS	Meteorological Sounding System
NASA	National Aeronautics and Space Administration
NCAR	National Center for Atmospheric Research
NOAA	National Oceanic and Atmospheric Administration
NSSL	National Severe Storms Laboratory
NWP	Numerical Weather Prediction
NWS MLB	National Weather Service in Melbourne, FL
PC	Personal Computer
PDF	Probability Density Function
QC	Quality Control
RAMS	Regional Atmospheric Modeling System
RAOB	Rawinsonde Observation
RH	Relative Humidity
RSA	Range Standardization and Automation

RUC	Rapid Update Cycle
RWO	Range Weather Operations
SB	Sea Breeze
SE	Standard Error
SLC-37	Space Launch Complex 37
SMC	Space and Missile Center
SMG	Spaceflight Meteorology Group
SRH	NWS Southern Region Headquarters
USAF	United States Air Force
UTC	Universal Coordinated Time
WMO	World Meteorological Organization
WWW	World Wide Web
XMR	CCAFS 3-letter identifier

Appendix A

AMU Projects	Milestones	Scheduled Begin Date	Scheduled End Date	Notes/Status
	AMU Project Schedule **31 October 2002**			
Statistical Forecast Guidance (Peak Winds)	Determine predictand(s)	Aug 01	Aug 01	Completed
	Data reduction, formulation and method selection	Sep 01	Mar 02	Completed
	Equation development, tests with independent data and individual cases	Mar 02	May 02	Delay 1 Month due to Customer Request for Further Analysis
	Prepare products, final report for distribution	May 02	Oct 02	Delay 1 Month due to Customer Request for Further Analysis
Land Breeze Forecasting	Data collection, data reduction, and QC	Aug 01	Nov 01	Completed
	Identification and analysis of case studies	Sep 01	Nov 01	Completed
	Development of land-breeze climatology	Dec 01	Apr 02	Completed
			Sep 02	Customer Request to Extend Analysis
	Development of forecast rules of thumb / automated tool	Apr 02	Jul 02	Completed
	Final report with forecasting rules of thumb	Jul 02	Oct 02	Customer Request to Extend Analysis
Improved Anvil Forecasting Phase III	Algorithm formulation and testing	Aug 02	Nov 02	On Schedule
	Memorandum	Dec 02	Dec 02	On Schedule
Extend Statistical Forecast Guidance to the SLF Towers	Create climatologies / determine theoretical distribution for 10-min peaks	Sep 02	Oct 02	On Schedule
	Develop PC-based tool to display climatologies and probabilities	Oct 02	Mar 03	On Schedule
	Prepare products, final report for distribution	Mar 03	May 03	On Schedule
Extend AMPS Moisture Analysis	Data collection, data reduction, and QC	Aug 02	Sep 02	On Schedule
	Analysis of humidity differences and impact on thunderstorm forecasting indices	Sep 02	Jan 03	On Schedule
	Memorandum	Feb 03	Apr 03	On Schedule

AMU Project Schedule 31 October 2002				
AMU Projects	Milestones	Scheduled Begin Date	Scheduled End Date	Notes/Status
MiniSODAR Evaluation	Data collection, data reduction, and QC	Aug 02	Jul 03	On Schedule
	Comparative analysis of miniSODAR and nearby wind tower observations	Sep 02	Jul 03	On Schedule
	Final Report	Jul 03	Sep 03	On Schedule
KSC-Funded Verification of Mesoscale NWP Models	Literature review	Mar 02	Mar 02	Completed
	Develop objective sea-breeze boundary detection algorithm	Apr 02	Aug 02	Completed
	Objective verification of RAMS sea-breeze boundaries	May 02	Dec 02	On Schedule
	Final report/Journal publications	Jan 03	Mar 03	On Schedule
LDIS Optimization and Training	Revise data ingest programs	Aug 02	Oct 02	On Schedule
	Provide recommendations for implementing new features in ADAS	Sep 02	Dec 02	On Schedule
	Training to SMG and NWS MLB personnel	Oct 02	Dec 02	On Schedule
	Memorandum	Oct 02	Dec 02	On Schedule

NOTICE